Electronic Supplementary Information: An arrayed high-content chemotaxis assay for patient diagnosis.

Erwin Berthier[1], Jill Surfus[2], James Verbsky[3], Anna Huttenlocher[2]& David Beebe[1]

[1]Wisconsin Institutes for Medical Research & Department of Biomedical Engineering, University of Wisconsin, 1111 Highland Av, Madison 53705, Wisconsin, USA. [2]Department of Pediatrics, University of Wisconsin, 1550 Linden Dr, Madison 53706, Wisconsin, USA. [3]Medical College of Wisconsin, 9000 W Wisconsin Ave, Milwaukee, Wisconsin, USA. Correspondence should be addressed to D.J.B (djbeebe@wisc.edu).

1. Different competing phenomena occurring in a passive pumping microchannel

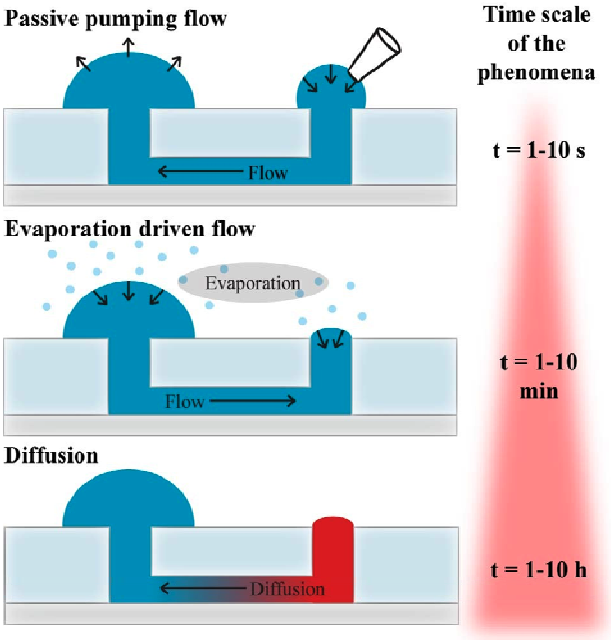

Different phenomena in a microchannel can cause the transport of soluble compounds from one port to another at wildly different timescales. Typical passive pumping flow occurs in seconds or less and is used to insert cells suspension or chemoattractants into the channel. Evaporation driven flow is a slower flow that transports liquid in a reverse direction to typical passive pumping. Diffusion is a weak transport mechanism that is easily disrupted.

When using PDMS an additional source of convection, and therefore disruption of the gradient, occurs by evaporation through the bulk material itself. This phenomenon is

particularly difficult to remedy as it occurs all throughout the channel. It is possible to reduce the magnitude of the evaporation with several approaches. First, a large portion of the evaporation occurs during the initial equilibration stage, during which the PDMS loads up with water vapor. To prevent this, prior to loading the chemoattractant, the microdevices can be soaked for 30 min in a warm environment. Despite these precautions, long term evaporation is difficult to prevent. Design features can be used to shield evaporation from the most critical parts the channel, in this case the gradient channel. The use of tall sacrificial channels winding around the features of interest have helped reduce unwanted evaporation further.

2. Most efficient ratio of resistance of optimal bypass function.

We explored different heights of the gradient channel, and quantified the level of convection by the distance fluorescent dye flowed into the gradient channel during insertion in the chemoattractant chamber. For ratios of 250 or more no significant displacement was observed. Overly thin channels, however, require increasingly high cell suspension densities to load the channel. The device presented here has a channel height of 50 um and length of 4 mm which was found to be a reasonable compromise.

Height (um)	Ratio	Diffusion/ Convection	Cell suspension density
25	2000	+++	4 million/mL
50	250	++	2 million/mL
100	30	-	1 million/mL

Ratio of resistances for different heights of channel. Proper dominance of diffusion increases with decreasing channel height. Inversely, the required cell suspension increases.

3. Different geometries and gradient characterization

The geometrical features of the source, sink and gradient channel also control how long a gradient can be maintained, as diffusive flux contributes in reducing the source concentration and increasing the source concentration. Different geometries have been developed with gradient channels 0.5, 1 and 2 mm long in order to reduce the time required to reach a steady, linear, gradient. As this setup time is proportional to the square of the channel's length, shorter gradient length, while decreasing the ratio of fluidic resistances, enable increasingly short setup times, down to minutes for a channel of 0.5mm in length. However, phase imaging is perturbed around the abrupt channel height change at the entrance of the channel making extremely short gradient channels unpractical to use. We found that channels of 1mm allow setup times of a few minutes while allowing good imaging qualities.

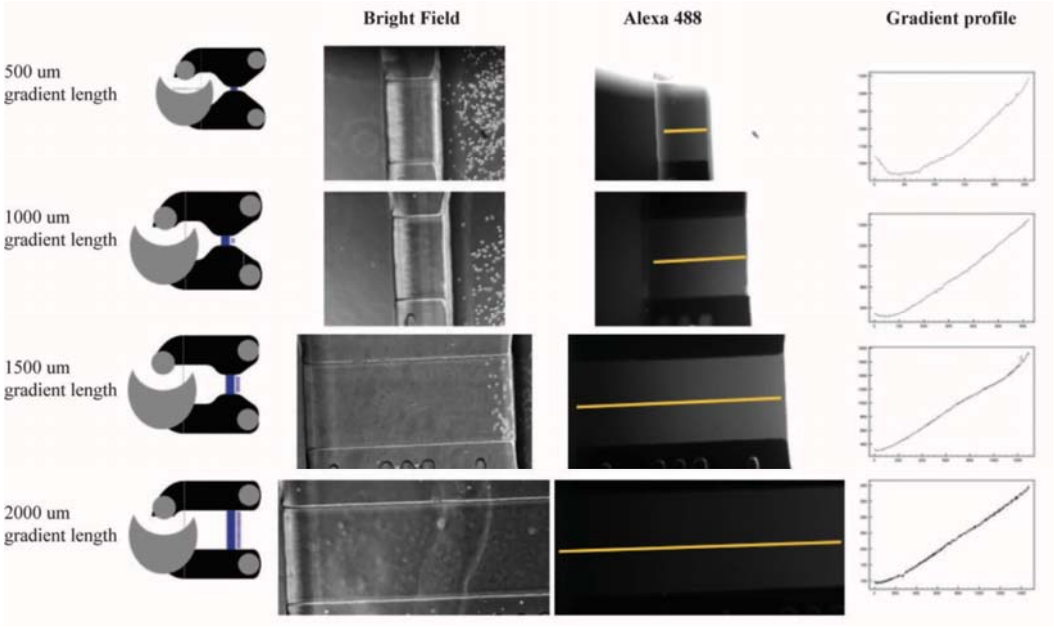

In addition, we developed different loading protocols to enable more functionality using these microdevices. The two protocols illustrated in the figure below describe how to load cells or solutions in the entire gradient channel and apply a gradient subsequently or how to pattern cells at a "starting" line. The first method is used to coat the channels with matrix proteins or image migrating cell at different values of the mean concentration through the gradient. The second method is useful to assess migration

characteristics in an assaying context. It ensures that all the cells start with the same observable gradient. It also enables to utilize these microdevices as end-point assays, without even requiring timelapse imaging. The readout then becomes extremely rapid and amendable to high-throughput, but more limited in content value.

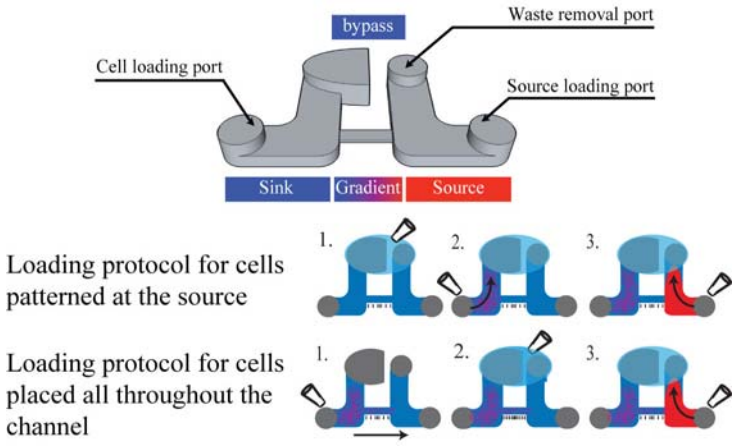

4. IL8 dose response of human primary neutrophils

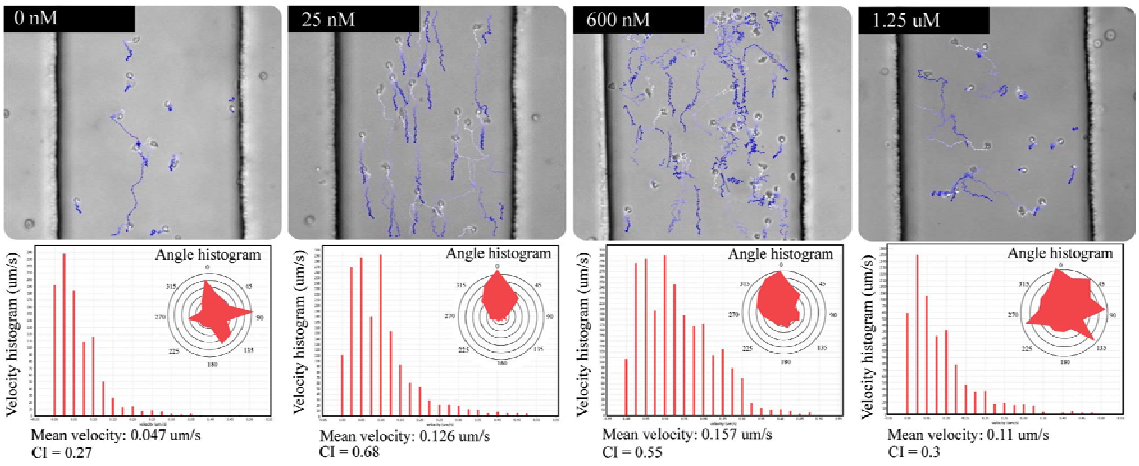

Human primary neutrophil dose response to increasing concentrations of IL-8 placed in the source reservoir. Cell migration was slow and steady at low concentration (25 nM) and rapid and random at high concentration (600 nM). At the highest source concentration (1.25 µM) neutrophils stopped migrating or exhibited reverse migration.

5. Convergence analysis

The conditions of convergence for the segmented analysis were explored further by the analysis of an array (6 rows and 10 columns) of similar generated random walks. For each row the same amount of segments were used for the analysis and used to measure the standard deviation of the measured value. This error decreases significantly with increasing number of segments until 150 both for the mean velocity and the segmented chemotaxis index, after which the decrease is lower, or negligible.

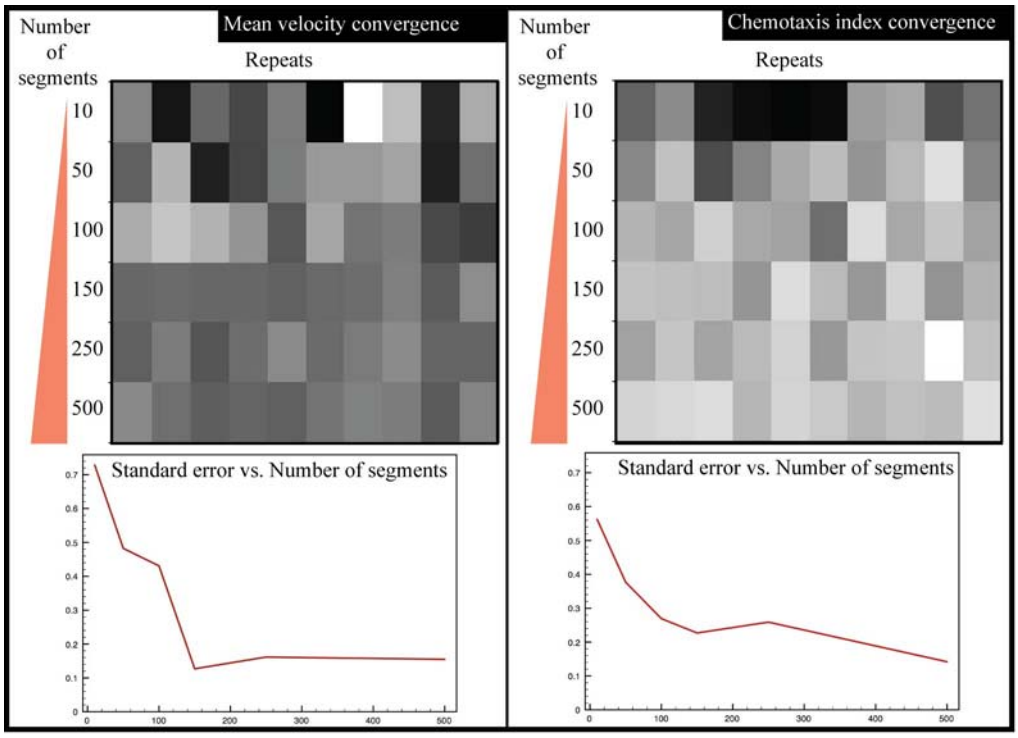

6. Rapid timelapse methods

Algorithms for automated cell tracking and analysis were developed to enable the exhaustive tracking of all cells migrating in the defined migration area in phase imaging. Using these techniques tracking of hundreds of cells is possible in minutes. In comparison, traditional tracking techniques use time-consuming manual or semi-manual methods allowing the tracking of only several cells chosen by the experimentator. The developed techniques, however, enable the exhaustive analysis of many cells over a short period of time, as opposed to few cells for a long period of time. By recording individual displacement vectors similar information can be extracted for mean velocity

and chemotaxis index by creating a segmented chemotaxis index, defined as the ratio of the area of the weighed angle polar histogram over the area of the disk corresponding to maximum velocity in all directions. We observe on experimental data of a dose response of human primary neutrophils to difference source gradients of IL8 that the traditional chemotaxis index and the segmented chemotaxis index vary consistently inversely. However that relationship was investigated further on a controlled set of data generated by simulation of a persistent random walk assimilated to migrating neutrophils.

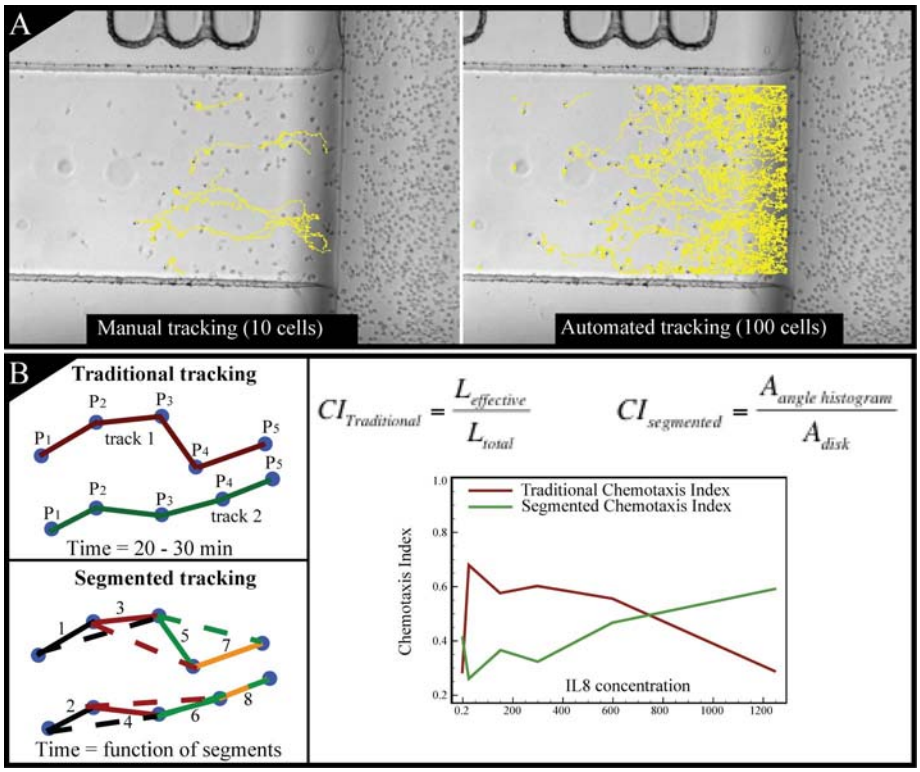

Persistent random walk tracks were simulated by computer and analysed using the algorithms developed for cell tracking analysis. An array of 18 random walk conditions (3 velocities, 6 angle variances) was simulated and analyzed. The results displayed good determination of the original characteristics of the tracks, with greater resolution for the velocity reading than the directionality. Overall, angle measurement is more complex at low velocities because of the noise induced by pixel bias. As any cell location is determined as an integer pixel position, the rounding error becomes more significant at

low migration velocities. Therefore, directionality can only reliably be compared for cell tracks of sufficient migration speed. Furthermore, the segmented chemotaxis index displays similar problems, as it is based on the angle histogram weighed by the mean velocity of the displacement. Thus, one must study the velocity readout prior to comparing chemotaxis index.

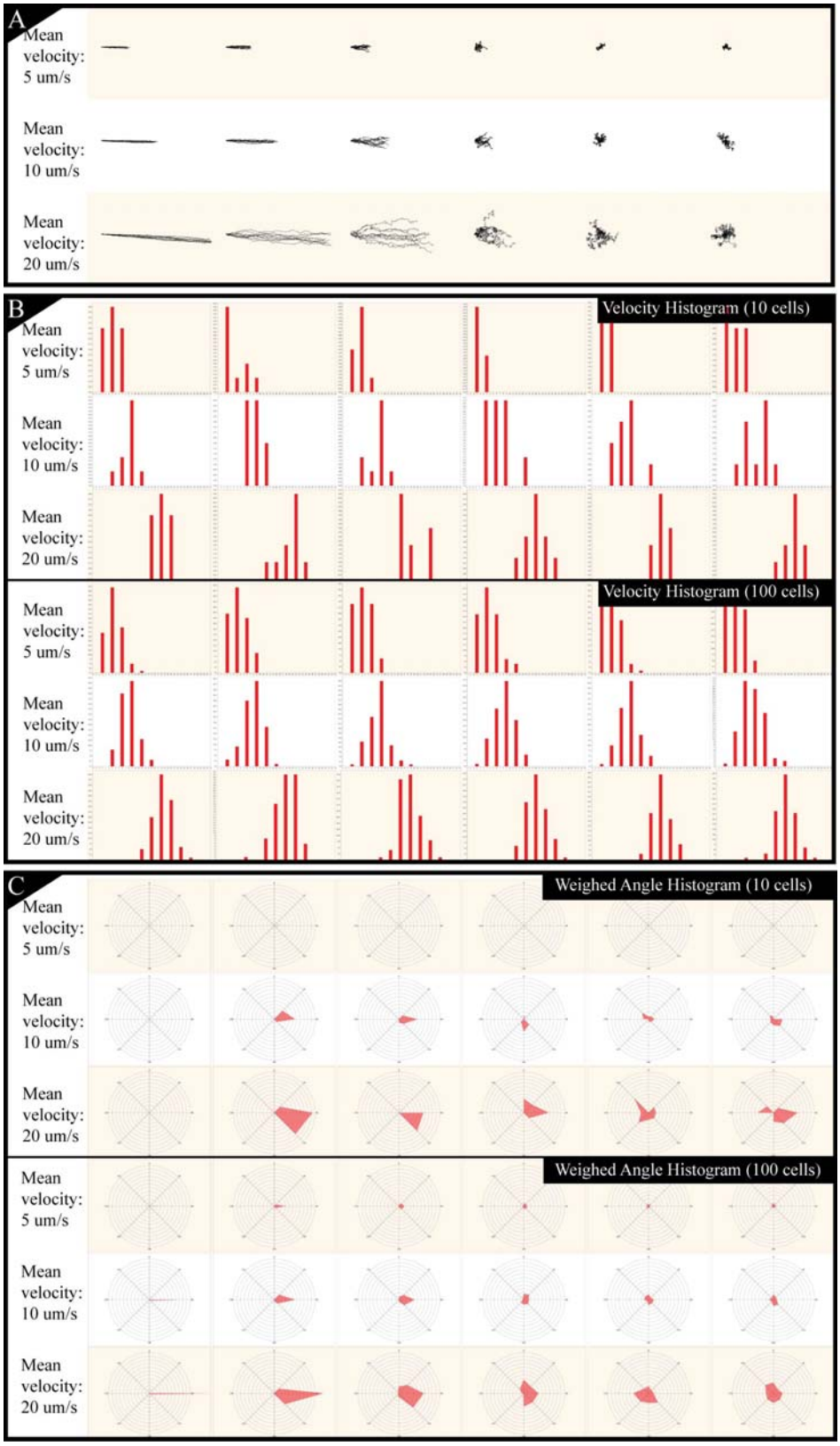

Higher throughput chemotaxis analysis opens the possibility of analysis outputs typically used in high-throughput screening, such as heat maps charts. Quantification of mean velocity and chemotaxis index have been plotted on a heat map to reveal the

effect of the number of segments used in the analysis and the correlation between the traditional chemotaxis index and the segmented chemotaxis index. First, we observe that as low as 10 segments may reveal velocity information (with significant noise) but not the directionality. Secondly, we observe that the segmented chemotaxis index varies consistently inversely to the traditional chemotaxis index, despite covering a smaller range of values. The CI typically varies from 0 to 1, whereas the SCI varies from 0.7 to 0.3, which is mainly attributed to the finite bins of the angular histogram.